

A Mutation in the *Drosophila melanogaster* eve Stripe 2 Minimal Enhancer Is Buffered by Flanking Sequences

Francheska López-Rivera,^{*,1,1} Olivia K. Foster Rhoades,^{*} Ben J. Vincent,^{*,2} Edward C. G. Pym,^{*} Meghan D. J. Bragdon,^{*,3} Javier Estrada,^{*,4} Angela H. DePace,^{*} and Zeba Wunderlich^{*,3,5}

^{*}Department of Systems Biology, Harvard Medical School, Boston, MA 02115, ¹GSAS Research Scholar Initiative, Harvard University, Cambridge, MA 02138 and ²Department of Developmental and Cell Biology, University of California, Irvine, CA 92697

ORCID IDs: 0000-0002-5160-6120 (F.L.-R.); 0000-0001-7782-7995 (O.K.F.R.); 0000-0003-4598-7016 (B.J.V.); 0000-0003-4301-5264 (M.D. J.B.); 0000-0003-3646-204X (J.E.); 0000-0001-5723-0438 (A.H.D.); 0000-0003-4491-5715 (Z.W.)

ABSTRACT Enhancers are DNA sequences composed of transcription factor binding sites that drive complex patterns of gene expression in space and time. Until recently, studying enhancers in their genomic context was technically challenging. Therefore, minimal enhancers, the shortest pieces of DNA that can drive an expression pattern that resembles a gene's endogenous pattern, are often used to study features of enhancer function. However, evidence suggests that some enhancers require sequences outside the minimal enhancer to maintain function under environmental perturbations. We hypothesized that these additional sequences also prevent misexpression caused by a transcription factor binding site mutation within a minimal enhancer. Using the *Drosophila melanogaster* even-skipped stripe 2 enhancer as a case study, we tested the effect of a Giant binding site mutation (gt-2) on the expression patterns driven by minimal and extended enhancer reporter constructs. We found that, in contrast to the misexpression caused by the gt-2 binding site deletion in the minimal enhancer, the same gt-2 binding site deletion in the extended enhancer did not have an effect on expression. The buffering of expression levels, but not expression pattern, is partially explained by an additional Giant binding site outside the minimal enhancer. Deleting the gt-2 binding site in the endogenous locus had no significant effect on stripe 2 expression. Our results indicate that rules derived from mutating enhancer reporter constructs may not represent what occurs in the endogenous context.

KEYWORDS

Drosophila melanogaster enhancer even-skipped transcription factor binding site

Developmental genes are often expressed in complex patterns in space and time. The instructions for these patterns are largely encoded in enhancers, stretches of DNA composed of transcription

factor (TF) binding sites. The earliest studies of enhancer function established that enhancers can retain their activity in synthetic reporter constructs, giving rise to the widely-held notion that enhancers are modules with distinct boundaries (Shlyueva *et al.* 2014). The idea that enhancers have distinct boundaries is reinforced by the way enhancers were traditionally identified – by reducing the DNA upstream of a gene's promoter into increasingly small fragments until a “minimal” enhancer that was sufficient to produce all or a subset of a gene's expression pattern was identified (Small *et al.* 1992). Even when using modern functional genomic methods, enhancers are annotated with finite boundaries and attempts are often made to identify the minimal enhancer (Arnold *et al.* 2013; Koenecke *et al.* 2016; Diao *et al.* 2017; Monti *et al.* 2017).

Minimal enhancer reporter constructs have been a powerful tool for studying transcriptional control. By mutating minimal enhancers in reporters, scientists have made key insights into evolution, DNA regulatory logic and the roles for transcription factor (TF) binding

Copyright © 2020 López-Rivera *et al.*

doi: <https://doi.org/10.1534/g3.120.401777>

Manuscript received August 1, 2020; accepted for publication October 1, 2020; published Early Online October 9, 2020.

This is an open-access article distributed under the terms of the Creative Commons Attribution 4.0 International License (<http://creativecommons.org/licenses/by/4.0/>), which permits unrestricted use, distribution, and reproduction in any medium, provided the original work is properly cited.

Supplemental material available at figshare: <https://doi.org/10.25387/g3.13010030>.

¹Present address: Department of Genetics, Harvard Medical School, Boston, MA 02115. ²Department of Biological Sciences, University of Pittsburgh, Pittsburgh, PA 15260. ³Department of Biomedical Engineering, Boston University, Boston, MA 02215. ⁴Novartis Institutes for Biomedical Research, Cambridge, MA 02139.

⁵Corresponding author: 4107 Natural Sciences 2, Irvine, CA 92697. E-mail: zeba@uci.edu

sites (Ney *et al.* 1990; Arnosti *et al.* 1996; Ma *et al.* 2000; Milewski *et al.* 2004; Crocker and Stern 2017). With the advent of high-throughput DNA synthesis and sequencing, this approach has been extended to study the effects of large numbers of enhancer variants in massively parallel reporter assays (Patwardhan *et al.* 2009; Melnikov *et al.* 2012; Inoue and Ahituv 2015; White 2015). An important, but often unstated assumption of this approach is that, if we assume that enhancers are modular, we can use minimal enhancer reporter measurements to decipher regulatory genetic variation in the intact genome. In other words, mutations would behave identically in an isolated enhancer and in the genome. Here, we set out to test this assumption directly.

There are several observations that enhancer function, particularly as defined by a minimal enhancer, may not be strictly modular (Spitz and Furlong 2012; Lim *et al.* 2018). When measured quantitatively, the expression patterns driven by some enhancer reporters do not precisely match the endogenous pattern (Staller *et al.* 2015). In many loci, the paradigm of a single enhancer driving expression in a single tissue is often an oversimplification. For example, in some loci, minimal enhancers cannot be identified for a given expression pattern, and many genes are controlled by seemingly redundant shadow enhancers (Barolo 2012; Sabaris *et al.* 2019). Furthermore, enhancer boundaries defined by DNase accessibility and histone marks often do not match minimal enhancer boundaries defined by activity in reporters (Kwasniewski *et al.* 2014; Henriques *et al.* 2018). In some cases, the minimal enhancer is sufficient for an animal's viability under ideal conditions, but sequences outside of the minimal enhancer are required for viability when the animal is exposed to temperature perturbations (Ludwig *et al.* 2011). Together, these examples highlight that while minimal enhancer regions can approximate the expression patterns of a gene, sometimes very closely, quantitative measurements of these regions' activities can reveal their inability to recapitulate the nuances of gene regulation in the endogenous context.

In this work, we directly test the assumption that the misexpression caused by a mutation in a minimal enhancer reporter construct will also be observed when the same mutation is found in the genome. We compared the changes in gene expression caused by a mutation in three versions of an enhancer: 1) a minimal enhancer in a reporter, 2) an extended enhancer that contains the minimal enhancer plus flanking sequences in a reporter, and 3) in the endogenous locus. If the minimal enhancer truly represents a modular functional enhancer unit, the effects of the mutation on gene expression will be the same in each of these contexts. If not, the effects caused by the mutation will differ.

We use the well-studied *Drosophila melanogaster even-skipped* (*eve*) stripe 2 enhancer as our case study for several reasons (Goto *et al.* 1989; Small *et al.* 1992). *Eve* encodes a homeodomain transcription factor essential for proper segment formation in *Drosophila*, and five well-characterized enhancers drive its seven-stripe expression pattern in the blastoderm embryo (Figure 1A). To understand the mechanism of *eve* stripe 2 enhancer function, classic experiments mutated transcription factor binding sites in minimal enhancer reporter constructs, resulting in a set of variants with known effects that we can test in an extended enhancer construct and in the endogenous locus (Small *et al.* 1992; Arnosti *et al.* 1996). Subsequent experiments showed that, while the *eve* stripe 2 minimal enhancer is sufficient for an animal's viability in *D. melanogaster*, the sequences outside of the minimal enhancer are required to drive robust patterns of gene expression when the animal is exposed to temperature perturbations (Ludwig *et al.* 2011), or to drive a proper stripe in

other species (Crocker and Stern 2017). Together, these experiments indicate that the minimal enhancer does not recapitulate the complete transcriptional control of *eve* stripe 2. The *Drosophila* blastoderm embryo also provides technical advantages; we can readily incorporate reporter constructs, make genomic mutations, and measure levels and patterns of gene expression at cellular resolution (Luengo Hendriks *et al.* 2006; Wunderlich *et al.* 2014). This allows us to measure potentially subtle differences in expression patterns and levels driven by different enhancer variants.

We hypothesized that a transcription factor binding site deletion will have its maximum effect on gene expression when found in a minimal enhancer, while its effects will be reduced, or buffered, when found in the extended enhancer and in the endogenous locus due to the contributions of additional regulatory DNA sequences. We tested our hypothesis and found that the effects of a Giant TF binding site deletion on gene expression are indeed buffered in the extended *eve* stripe 2 enhancer and in the endogenous locus. This buffering is partially explained by an additional Giant binding site in the sequence outside the *eve* stripe 2 minimal enhancer. These results imply that we cannot always extrapolate the effects of naturally or experimentally induced enhancer mutations in minimal reporters to extended sequences or to the endogenous intact locus. We discuss implications of our results for studying the functional consequences of regulatory sequence variation.

MATERIALS AND METHODS

Enhancer sequences and mutations in reporter constructs

Each of the *eve* stripe 2 enhancer sequences was cloned into a pB ϕ Y plasmid containing an *eve* basal promoter-*lacZ* fusion gene, the *mini-white* marker, and an attB integration site. The enhancer sequences are located immediately upstream of the *eve* basal promoter. All constructs were integrated by Genetic Services, Inc. into the attP2 docking site of the *Drosophila melanogaster* γ [1], w [67c23] line. We followed the *mini-white* eye marker as we conducted crosses to make the transgenic fly lines homozygous.

The 484 base pair (bp) wild-type minimal (minWT) enhancer sequence was defined by Small and colleagues (Small *et al.* 1992). Min Δ gt-2 is the minWT enhancer with a 43 bp deletion of the giant-2 (gt-2) binding site as described in (Small *et al.* 1992). The wild-type extended (extWT) enhancer is the minWT sequence plus the 50 bp upstream and 264 bp downstream flanking sequences present in the *eve* locus. The boundaries of the extWT enhancer are two conserved blocks of 18 and 26 bp on the 3' and 5' ends of the enhancer (Ludwig *et al.* 1998). The ext Δ gt-2 enhancer consists of the extWT enhancer with the same gt-2 binding site deletion as in min Δ gt-2.

To computationally predict additional Gt sites in the extended enhancer, we used PATSER and three different Gt position weight matrices (PWMs) generated with data from yeast one-hybrid, DNA footprinting, and SELEX assays (Hertz and Stormo 1999; Noyes *et al.* 2008; Li *et al.* 2011; Schroeder *et al.* 2011). A common Gt binding site, which we named gt-4, was found in the downstream flanking sequence of the extended enhancer using all three PWMs with a p-value of 0.001 (Figure S1). Because of overlaps with other predicted binding sites, the gt-4 binding site was mutated by changing five nucleotides in ext Δ gt-2 to create the ext Δ gt-2, Δ gt-4 enhancer.

The minWT-sp1 and minWT-sp2 enhancers consist of the minWT enhancer and two different 264 bp downstream spacer sequences, sp1 and sp2. Each of these sequences are about half of a 500 bp *lacZ* sequence from which we removed high affinity binding

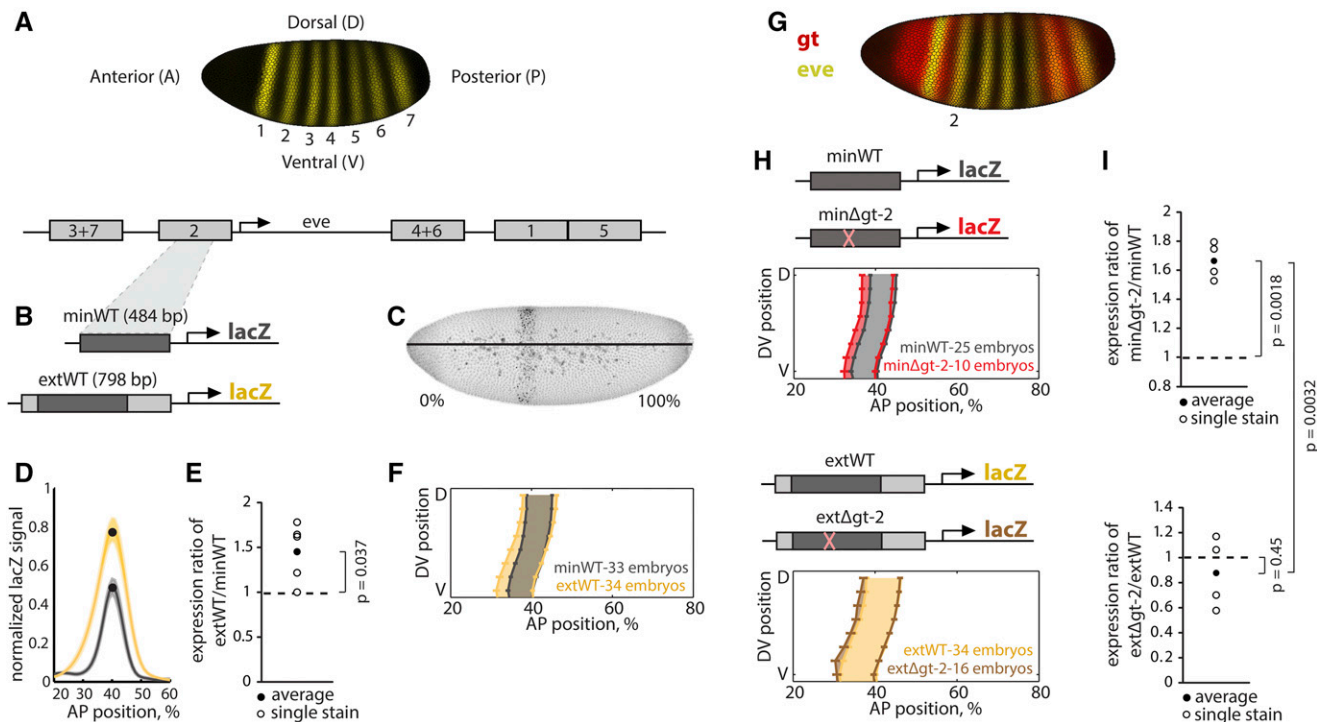


Figure 1 The effect of the *gt-2* binding site mutation is buffered in the *eve* stripe 2 extended enhancer. (A) *Eve* is expressed as a pattern of seven stripes along the anterior-posterior axis of the *Drosophila melanogaster* blastoderm, and this pattern is driven by five enhancers. Here we show a visual rendering of *even-skipped* expression as measured in (Fowlkes et al. 2008). (B) We generated transgenic reporter fly lines with the wild-type minimal (minWT) and extended (extWT) *eve* stripe 2 enhancers, and we measured *lacZ* expression in embryos using *in situ* hybridization. (C) A representative image of a minWT reporter embryo stained for *lacZ* and a normalization gene, *hkb*, is shown. The image shown is a maximum intensity projection. (D) We plotted *lacZ* levels in a lateral strip of cells along the AP axis (as shown in C) for the minWT (dark gray) and extWT (yellow) enhancers measured in a single stain, with the shading showing the standard error of the mean. The extWT enhancer drives a higher peak level of expression. (E) We calculated the ratio of peak *lacZ* expression levels (black dots in D) driven by the extWT and minWT enhancers in five different stains (open circles). The average ratio of the five stains is represented by a closed circle. The extWT enhancer drives 1.45 times higher expression than the minWT ($p(\frac{\text{extWT}}{\text{minWT}}=1) = 0.037$, one-sample t-test). (F) We show the average boundary positions of the *lacZ* expression pattern. Error bars show standard error of the mean boundary positions of the expression pattern. The extWT enhancer drives a wider pattern of expression (yellow shading) than the minWT enhancer (gray shading), with the anterior border of the stripe laying ~ 1.6 cell widths more anterior than the minWT enhancer pattern. (G) The transcription factor Giant (Gt) is expressed as a broad band anterior to *eve* stripe 2 and represses *eve*, establishing the anterior boundary of stripe 2. We have included a visual rendering of Giant protein and *even-skipped* mRNA during early nuclear cycle 14 of the blastoderm stage as measured in (Fowlkes et al. 2008). (H, I) We characterized the expression patterns and levels driven by the minimal (minΔgt-2, top panels) and extended (extΔgt-2, bottom panels) enhancers with a *gt-2* binding site deletion. In the minΔgt-2 enhancer, the *gt-2* deletion causes an anterior shift in the anterior boundary of the expression pattern and an increase in expression level ($p(\frac{\text{min}\Delta\text{gt-2}}{\text{minWT}}=1) = 0.0018$, one-sample t-test). In the extended enhancer, the *gt-2* deletion causes a very slight shift in the anterior boundary and no significant change in peak expression level ($p(\frac{\text{ext}\Delta\text{gt-2}}{\text{extWT}}=1) = 0.45$, one-sample t-test; $p(\frac{\text{ext}\Delta\text{gt-2}}{\text{extWT}} > \frac{\text{min}\Delta\text{gt-2}}{\text{minWT}}) = 0.0032$, one-sided, two-sample t-test with unequal variances).

sites for Bicoid, Hunchback, Giant, and Kruppel, using a PATSER p-value of 0.003. The minΔgt-2-sp1 enhancer is composed of minΔgt-2 and sp1. MinΔgt-2-sp1+gt-4 is the minΔgt-2-sp1 enhancer containing the additional *gt-4* binding site that we identified, located in the position where it is found in the extended enhancer. File S1 contains the sequences of all the enhancers that were tested in reporter constructs.

Endogenous *eve* giant-2 deletion using the CRISPR system

Briefly, gRNAs (5'-TCTAACTCGAAAGTGAAACGAGG-3' and 5'-ATTCCGTCTAAATGAAAGTATGG-3') adjacent to the *gt-2* binding site were cloned into pU6-BbsI-chiRNA. A ScarlessDsRed selection cassette (<https://flycrispr.org/scarless-gene-editing/>) was used with ~ 500 bp homology arms flanking the gRNA cut sites in the *eve* stripe 2 enhancer. These plasmids were injected into $y[1] w[67c23]; attP2[\text{nos-Cas9}]$ by BestGene. The dsRed selection cassette

was mobilized by crossing to $w[1118]; In(2LR)Gla, wg[Gla-1]/CyO; Herm\{3xP3\text{-}ECFP, \text{alphatub-piggyBacK10}\}M10$, and selecting for non-dsRed eyed flies, to give the final allele *eve[eveS2Δgt-2]*. Further crosses to remove the transposase yielded flies with the genotype $w[1118]; eve[eveS2\Delta\text{gt-2}]$, which we term “Δgt-2 *eve* locus.” The edit was confirmed by PCR. The control flies to which the CRISPR flies were compared had the genotype $y[1] w[67c23]; attP2[\text{hbP2-LacZ}]$.

In situ hybridization and imaging

We collected and fixed 0-4 hr old embryos grown at 25°, and we stained them using *in situ* hybridization as in (Luengo Hendriks et al. 2006; Wunderlich et al. 2014). We incubated the embryos at 56° for two days with DNP-labeled probes for *hkb* and DIG-labeled probes for *ftz*. Transgenic reporter embryos were also incubated with a DNP-labeled probe for *lacZ*, and the WT *eve* locus and Δgt-2 *eve* locus CRISPR embryos were incubated with a DNP-labeled probe for *eve*.

Hkb probes were used to normalize *lacZ* expression levels between the different transgenic reporter lines. The DIG probes were detected with anti-DIG-HRP antibody (Roche, Indianapolis, IN) and a coumarin-tyramide color reaction (Perkin-Elmer, Waltham, MA), and the DNP probes were detected afterward with anti-DNP-HRP (Perkin-Elmer) antibody and a Cy3-tyramide color reaction (Perkin-Elmer). Embryos were treated with RNase and nuclei were stained with Sytox green. We mounted the embryos in DePex (Electron Microscopy Sciences, Hatfield, PA), using a bridge of #1 slide coverslips to avoid embryo morphology disruption.

Reporter embryos from the early blastoderm stage (4–10% membrane invagination, roughly 10–20 min after the start of the blastoderm stage) were imaged, and CRISPR embryos from early blastoderm stage (9–15% membrane invagination, roughly 15–25 min after the start of the blastoderm stage) were imaged. We used 2-photon laser scanning microscopy to obtain z-stacks of each embryo on a LSM 710 with a plan-apochromat 20X 0.8 NA objective. Representative images are shown in Figure S2. Each stack was converted into a PointCloud, a text file that includes the location and levels of gene expression for each nucleus (Luengo Hendriks *et al.* 2006).

Data analysis of eve stripe 2 reporter constructs

To normalize the *lacZ* levels in the reporter embryos, we divided the *lacZ* signal by the 95% quantile of *hkb* expression in the posterior 10% of each embryo (Wunderlich *et al.* 2014). We expect the *lacZ* and *hkb* levels to be correlated within a transgenic line. To verify this, we ran a regression of the 99% quantile *lacZ* value from each embryo and the 95% quantile *hkb* value. Cook's distance was used to discard influential outliers (on average, 26.5% of analyzed embryos) (Wunderlich *et al.* 2014). To avoid extraneous sources of noise in the normalization, we only compared *lacZ* levels between embryos with the same genetic background and stained in the same *in situ* hybridization experiment.

To calculate the average *lacZ* expression levels along the anterior-posterior (AP) axis in each transgenic line, we used the `extractpattern` command in the PointCloud toolbox. This command divides the embryo into 16 strips around the dorso-ventral (DV) axis of the embryo, and for each strip, calculates the mean expression level in 100 bins along the anterior-posterior (AP) axis. We averaged the strips along the right and left lateral sides of the embryos and subtracted the minimum value along the axis to remove background noise.

We calculated the peak average *lacZ* expression level within the *eve* stripe 2 region for each transgenic line in each *in situ* experiment separately. We then calculated the ratio between the peak average *lacZ* expression levels of two transgenic lines stained in the same *in situ* experiment. Ratios were calculated for each stain and the average ratio from multiple stains was determined (see Figure S3 for details of stain numbers and sample sizes). To compare ratios to 1, we used one-sample *t*-tests. To compare two different ratios to each other, we used two-sample *t*-tests with unequal variances.

The boundaries of *eve* stripe 2 expression were defined as the inflection point of the *lacZ* expression levels. Since the boundaries of *lacZ* expression should not change between stains, plots with the average boundaries of *lacZ* expression in each transgenic line were made with embryos pooled from multiple stains (see Figure S3 for number of embryos measured for each genotype). The cell length differences were calculated by determining the average position of the boundary across the DV axis of the embryos analyzed. One cell length is approximately equivalent to one percent of the embryo length.

Data analysis of endogenous eve stripe 2 giant-2 deletion

Briefly, we normalized to *eve* stripe 1 cellular expression to compare *eve* levels in the *eve*[*eveS2Δgt-2*] embryos and the control (Fowlkes *et al.* 2008). As described above, using the `extractpattern` command from the PointCloud toolbox, we found an averaged lateral trace across both sides of the embryo. The peak average *eve* expression for each stripe was normalized to the peak average expression of *eve* stripe 1. We performed a comparison of stripe levels between conditions using a two-sided rank sum test.

The boundary of *eve* stripes were defined as above using `extractpattern` and, for a given embryo, eight boundary positions on the left and right lateral sides were averaged. Plots with the average boundary of *eve* stripe 2 in the *eve*[*eveS2Δgt-2*] vs. control were made with embryos pooled from different stains. To compare boundaries between the two genotypes, a Mann-Whitney U Test was used, with the factors being one of the eight dorso-ventral positions along both lateral sides of the embryo and the embryo genotype. The p-value was corrected using a Bonferroni adjustment and reported for the genotype factor effect.

Data availability

All transgenic and CRISPR fly lines are available upon request. Supplemental files are available at FigShare. File S1 contains the sequences for all enhancer constructs, and Files S2 and S3 have binding site locations for the diagrams in Figure S6. Figure S1 has a depiction of all the predicted Gt binding sites in the *eve* stripe 2 enhancer. Figure S2 has representative images for all the genotypes analyzed. Figure S3 contains all ratios presented in Figures 1–3 in one plot. Figure S4 has details on the normalization used for the CRISPR fly data analysis. Figure S5 has the expression patterns for the other *eve* stripes in the *eve*[*eveS2Δgt-2*] CRISPR flies. Figure S6 contains the enhancer sequence of the *eve*[*eveS2Δgt-2*] locus as well as a map of the predicted binding sites. Figure S7 contains a multi-species comparison of the *eve* stripe 2 enhancer. Table S1 describes all the individual embryos analyzed in this project, and File S4 contains the PointCloud files for each embryo, which includes the positions of all the nuclei in each embryo and the expression values for therein. Supplemental material available at figshare: <https://doi.org/10.25387/g3.13010030>.

RESULTS

The minimal and extended eve stripe 2 enhancers drive different patterns and levels of expression

To test the effects of mutations in the minimal and extended *eve* stripe 2 enhancer on expression, we began by characterizing the wild-type (WT) expression patterns driven by the previously-defined minimal (minWT) and extended (extWT) enhancers (Figure 1B–F). The minimal enhancer is 484 bp and was identified as the smallest piece sufficient to drive expression in the region of stripe 2 (Small *et al.* 1992). The extended enhancer boundaries were chosen as the two conserved blocks of 18 and 26 bp on the 3' and 5' sides of the minimal enhancer, resulting in a 798 bp piece (Ludwig *et al.* 1998). We generated transgenic animals with *lacZ* reporter constructs inserted into the same location of the genome, and we measured *lacZ* expression using *in situ* hybridization and a co-stain for normalization (Wunderlich *et al.* 2014). Embryos in the first quarter of nuclear cycle 14 (nc-14) were analyzed because our normalization technique is most accurate during this time period (Wunderlich *et al.* 2014). Moreover, key *eve* regulators, including Giant, are expressed by this

time (Petkova *et al.* 2019). The stripe driven by the extended enhancer is wider – its anterior boundary is ~ 1.6 cell widths more anterior than that of the minimal enhancer (Figure 1F). In addition, the peak *lacZ* expression driven by the extWT is 1.45 times higher than the minWT enhancer (p-value = 0.037, one-sample *t*-test comparing extWT/minWT ratio to 1; Figure 1D, E).

The *gt-2* transcription factor binding site deletion is buffered in the extended enhancer

To test the effect of mutations in the minimal and extended enhancers, we looked to the literature to find a known sequence mutation that had a measurable effect on expression in the minimal enhancer. Previous work identified three footprinted binding sites within the minimal enhancer for the repressor Giant (Gt), which is expressed anterior of *eve* stripe 2 (Small *et al.* 1992) (Figure 1G). A minimal enhancer with a deletion of one of these binding sites, *gt-2*, drives higher and broader anterior expression than the WT enhancer (Arnosti *et al.* 1996).

We chose to focus our work on *gt-2* instead of the other Giant binding sites for two reasons: (1) we wanted to only mutate one TF binding site to best simulate natural population variation and (2) deletion of *gt-2* resulted in the greatest effect of *eve* stripe 2 expression (Arnosti *et al.* 1996). We created reporters with the same deletion of *gt-2* as in Arnosti *et al.* 1996 in the minimal and extended enhancers (Figure 1H) and measured the effect of the deletion on both expression levels and patterns. Consistent with previous results, we found that min Δ *gt-2* drives 1.67 times the expression of the minWT enhancer (p-value = 0.0018, one-sample *t*-test comparing min Δ *gt-2*/minWT ratio to 1, in Figure 1I, top), and a pattern that is expanded 1.7 cell widths to the anterior (Figure 1H, top). Notably, in the Arnosti *et al.* (1996) study, the authors observed a large anterior expansion in *eve* stripe 2 when *gt-2* was deleted in mid-blastoderm embryos. In early blastoderm embryos, we observe a more modest anterior expansion. The more modest expansion is likely because we are collecting data when Gt levels are lower and prior to *eve* expression refinement, when *eve* stripe 2 shifts to the posterior (Petkova *et al.* 2019).

In contrast, the expression level driven by the ext Δ *gt-2* enhancer is not significantly different from the extWT enhancer (p-value = 0.45, one-sample *t*-test comparing ext Δ *gt-2*/minWT ratio to 1; Figure 1I, bottom), and the pattern is expanded by only 0.9 cell widths (Figure 1H, bottom). The min Δ *gt-2*/minWT expression ratio is also significantly larger than the ext Δ *gt-2*/extWT ratio (p-value = 0.0032, one-sided, two-sample *t*-test with unequal variances comparing min Δ *gt-2*/minWT to ext Δ *gt-2*/extWT), indicating that the deletion has a much larger effect on the expression level driven by the minimal enhancer than by the extended enhancer. Together, these results indicate that the effect of the *gt-2* binding site deletion is buffered in the extended enhancer.

Distance from the promoter reduces expression levels and does not explain buffering

The minimal and extended enhancers differ from one another in the flanking sequences. These flanks may contribute to buffering in two primary ways: 1) the flanks may contain TF binding sites or other specific sequence elements, and 2) the flanks increase the distance of the minimal piece from the promoter.

In the minWT constructs the enhancer is 38 bp from the promoter, whereas in the extWT constructs the same minWT sequence is located 302 bp away from the promoter. To test if this change in distance contributes to the differences in expression of the two

constructs, we inserted two different 264 bp spacer sequences (sp1 and sp2) into the minWT reporters, to make the constructs minWT-sp1 and minWT-sp2 (Figure 2A). The two distinct spacers, sp1 and sp2 are *lacZ* sequences from which high affinity binding sites for the best known regulators involved in *eve* stripe 2 expression have been removed. For both spacers, increasing the distance of the minWT sequence significantly reduces expression levels, (sp1: p-value = 3.6e-4; sp2: p-value = 5.0e-4, one-sample *t*-tests comparing each ratio to 1; Figure 2C), while only minimally affecting the AP positioning. The anterior and posterior boundaries of the minWT-sp1 are shifted to the posterior part of the embryo by 1.4 and 1.3 cell lengths, respectively, when compared to minWT (Figure 2B). The anterior and posterior boundaries of minWT-sp2 are shifted to the posterior by 1.0 and 1.1 cell lengths, respectively, when compared to minWT (Figure 2B). These data demonstrate that the level of expression driven by minWT is influenced by enhancer-promoter distance.

To test if promoter-enhancer distance explains the buffering of the *gt-2* deletion, we made a construct with the min Δ *gt-2* enhancer separated from the promoter by sp1, min Δ *gt-2*-sp1, and compared it to minWT-sp1 (Figure 2D). If the distance from the promoter contributes to the buffering effect, the expression ratio of min Δ *gt-2*-sp1/minWT-sp1 would be smaller than that of min Δ *gt-2*/minWT, and the spatial pattern between minWT-sp1 and min Δ *gt-2*-sp1 would be more similar than between minWT and min Δ *gt-2*. In fact, the opposite is true – the ratio is larger (p-value = 0.0025, one-sided, two-sample *t*-test with unequal variances comparing min Δ *gt-2*-sp1/minWT-sp1 to min Δ *gt-2*/minWT), and the spatial pattern is different (Figure 2E, F). This finding is surprising and suggests a change in regulatory information integration when both *gt-2* is deleted and the enhancer-promoter distance is increased (see Discussion). Together this indicates that the relative distance of the core 484 bp to the promoter does not contribute to the buffering in the extended piece.

An additional Gt binding site in the flanking sequence partially explains the buffering

Since promoter-enhancer distance does not explain the buffering of the extended enhancer, the buffering must be due to differences in the sequence content of the minimal and extended enhancers. We hypothesized that there might be additional Gt binding sites in the flanks of the extended enhancer that explain the observed buffering of the *gt-2* deletion. We scanned these flanking regions with three existing Gt position weight matrices (PWMs) and found one binding site downstream of the minWT sequence that was common to all the PWMs, which we call *gt-4*. We suspected this site was most likely to be bound *in vivo* (see Materials and Methods and Figure S1). We mutated the common site to make the ext Δ *gt-2*, Δ *gt-4* construct (Figure 3A). If this common site contributes to buffering, we would expect that the ext Δ *gt-2*, Δ *gt-4* construct would drive higher expression levels and a wider stripe than the extWT construct. The ext Δ *gt-2*, Δ *gt-4* enhancer drives a pattern with an anterior boundary that is not significantly different from the ext Δ *gt-2* enhancer (Figure 3B). However, compared to the peak expression levels driven by the extWT enhancer, the ext Δ *gt-2*, Δ *gt-4* enhancer drives 1.2 times more expression (p-value = 0.065, one-sample *t*-test comparing ext Δ *gt-2*, Δ *gt-4*/extWT ratio to 1) (Figure 3C). Because the peak expression ratio of ext Δ *gt-2*, Δ *gt-4*/extWT is between that of min Δ *gt-2*/minWT and ext Δ *gt-2*/extWT, this result suggests that the additional *gt-4* binding site is partially responsible for buffering the effect of the *gt-2* deletion on expression levels (Figure S1). However, since the ext Δ *gt-2* and ext Δ *gt-2*, Δ *gt-4* enhancers drive

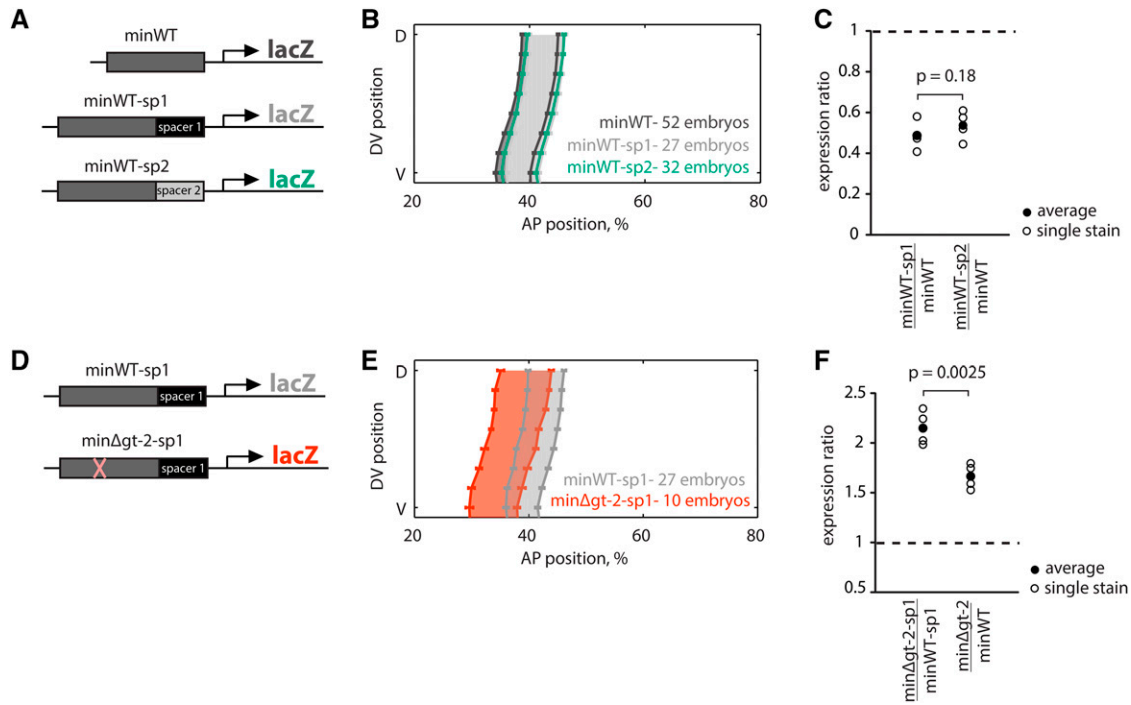


Figure 2 Distance from the promoter reduces *eve* stripe 2 expression levels and is not sufficient to explain the buffering. (A) To test if distance from the promoter contributes to buffering the *gt-2* deletion, we used two different 264 bp spacer sequences (sp1 and sp2) to make two constructs, minWT-sp1 and minWT-sp2. (B) We find that moving the minimal enhancer away from the promoter slightly shifts the boundaries of the stripe to the posterior. Error bars show standard error of the mean boundary positions of the expression pattern. (C) A comparison of peak expression levels shows that moving the minimal enhancer away from the promoter reduces peak expression levels in both spacer constructs ($p(\frac{\text{minWT-sp1}}{\text{minWT}} > 1) = 3.6 \text{ e-}4$, $p(\frac{\text{minWT-sp2}}{\text{minWT}} > 1) = 5.0 \text{ e-}4$; one-sided, one-sample *t*-test; $p(\frac{\text{minWT-sp1}}{\text{minWT}} > \frac{\text{minWT-sp2}}{\text{minWT}}) = 0.18$; one-sided, two-sample *t*-tests with unequal variances). (D) We tested if distance from the promoter is sufficient to explain the *gt-2* site deletion buffering in the extended enhancer by introducing the *gt-2* site deletion into the minWT-sp1 construct, minΔgt-2-sp1. (E) The minΔgt-2-sp1 construct drives an expression pattern that is dramatically shifted to the anterior, indicating that the spacer cannot buffer the *gt-2* binding site deletion's effect on expression pattern. (F) The minΔgt-2-sp1/minWT-sp1 peak expression ratio is significantly larger than minΔgt-2/minWT ratio, indicating that the *gt-2* deletion has a more dramatic effect in the minΔgt-2-sp1 and that increasing distance from the promoter does not buffer the effects of the *gt-2* deletion ($p(\frac{\text{minΔgt-2-sp1}}{\text{minWT-sp1}} = 1) = 9.3 \text{ e-}4$, one-sample *t*-test; $p(\frac{\text{minΔgt-2-sp1}}{\text{minWT-sp1}} < \frac{\text{minΔgt-2}}{\text{minWT}}) = 0.0025$, one-sided, two-sample *t*-test with unequal variances).

virtually the same expression pattern, this binding site is not responsible for buffering the effect of *gt-2* deletion on expression pattern. Therefore, this additional *gt-4* binding site can only partially explain why the extended enhancer can buffer the effect of the *gt-2* deletion. Additional Gt binding sites, other TF binding sites, or other functional sequences in the extended enhancer sequence flanks may be responsible for the unexplained buffering (see Discussion).

Adding a Gt binding site to the minimal enhancer is not sufficient to buffer a Gt mutation

Since the additional *gt-4* site is necessary to partially buffer the *gt-2* deletion, we wanted to test whether it was also sufficient. We inserted the additional *gt-4* binding site into the spacer of the minΔgt-2-sp1 construct in the same position as *gt-4* in the extWT construct to make the minΔgt-2-sp1+*gt-4* construct (Figure 3D). We compared its expression to the minWT-sp1 and the minΔgt-2-sp1 constructs. If the additional *gt-4* site is sufficient to buffer the *gt-2* deletion, we would expect that the minΔgt-2-sp1+*gt-4* would drive lower expression levels than minΔgt-2-sp1 and a similar expression pattern to the minWT-sp1 construct. We found that the peak expression ratio of minΔgt-2-sp1+*gt-4*/minWT-sp1 is on average lower, but not significantly different from the minΔgt-2-sp1/minWT-sp1 ratio,

indicating that this binding site alone is not sufficient to buffer the *gt-2* deletion (*p*-value = 0.17, one-sided, two-sample *t*-test with unequal variances) (Figure 3F). The expression patterns driven by minΔgt-2-sp1+*gt-4* and minΔgt-2-sp1 are also very similar, though there is a slight posterior shift of the anterior boundary in the minΔgt-2-sp1+*gt-4* construct (Figure 3E). It is possible that this *gt-4* binding site needs its original context to function properly, which may be due to the importance of binding site flanks on DNA shape (Rohs *et al.* 2010; Li and Eisen 2018), or other, unknown requirements.

The *gt-2* transcription factor binding site mutation is buffered in the endogenous locus

To test whether the *gt-2* deletion can be buffered in the intact locus, as it is in the extended enhancer, we used CRISPR editing to generate flies homozygous for the same *gt-2* deletion in the endogenous *eve* locus, which we called Δgt-2 *eve* locus (Figure 4A, Figure S6). We then measured *eve* expression patterns and levels using *in situ* hybridization in the Δgt-2 *eve* locus embryos and WT *eve* locus embryos (see Methods for details). To measure expression levels in *eve* stripe 2, we internally normalized to the levels of *eve* stripe 1, which is the first *eve* stripe to be expressed in this developmental stage (Figure S4; see

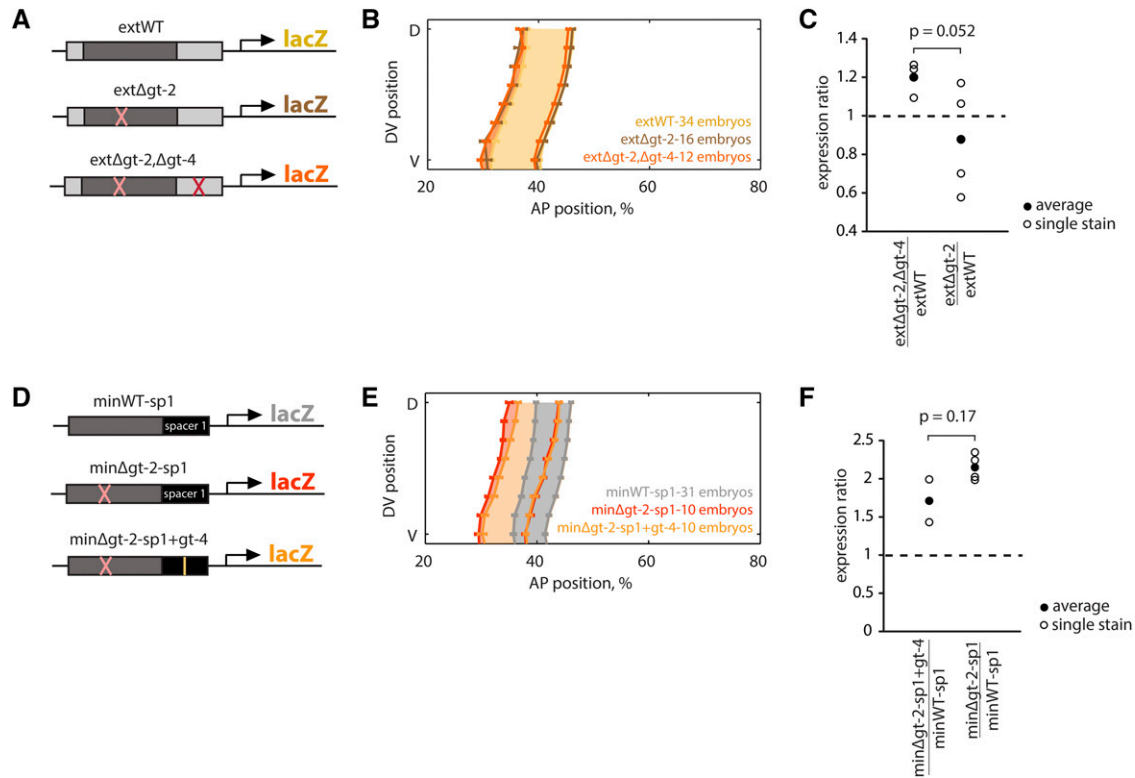


Figure 3 An additional Gt binding site partially explains the buffering. (A) We found an additional predicted Gt binding site outside the minimal enhancer sequence but within the extended enhancer, which we called *gt-4*. A reporter construct, *extΔgt-2,Δgt-4*, testing for the necessity of the additional Gt binding site was made by mutating the predicted *gt-4* binding site. (B) The average position of the *lacZ* anterior boundaries was nearly identical for the *extΔgt-2* and *extΔgt-2,Δgt-4* constructs, indicating that eliminating the additional *gt-4* binding site does not affect buffering of the *gt-2* deletion on expression pattern. Error bars show standard error of the mean boundary positions of the expression pattern. (C) If the additional *gt-4* site was necessary and sufficient for the buffering, the *extΔgt-2,Δgt-4*/*extWT* ratio would be higher than 1 and very similar to *minΔgt-2*/*minWT* ratio. If the additional *gt-4* binding site was not necessary at all, the *extΔgt-2,Δgt-4*/*extWT* ratio would be similar to 1 and to the *extΔgt-2*/*extWT* ratio. The results suggest that the additional *gt-4* site explains only some of the buffering of the *gt-2* deletion on expression level ($p(\frac{\text{ext}\Delta\text{gt-2},\Delta\text{gt-4}}{\text{extWT}} < \frac{\text{ext}\Delta\text{gt-2}}{\text{extWT}}) = 0.065$, one-sample t-test; $p(\frac{\text{ext}\Delta\text{gt-2},\Delta\text{gt-4}}{\text{extWT}} < \frac{\text{ext}\Delta\text{gt-2}}{\text{extWT}}) = 0.052$, one-sided, two-sample t-test with unequal variances). (D) We tested the sufficiency of the additional *gt-4* binding site by making a construct with the *minΔgt-2-sp1* element and inserting the additional *gt-4* binding site in the same position relative to the promoter as in the extended enhancer (*minΔgt-2-sp1+gt*). (E) The additional *gt-4* binding site shifts the anterior boundary of expression slightly to the posterior, when compared to the pattern driven by *minΔgt-2-sp1*. (F) The peak *minΔgt-2-sp1+gt-4*/*minWT-sp1* ratio is lower, but not significantly different from the *minΔgt-2-sp1*/*minWT-sp1* ratio, indicating that this *gt-4* binding site is not sufficient to explain the buffering of expression level in the extended enhancer ($p(\frac{\text{min}\Delta\text{gt-2-sp1+gt-4}}{\text{minWT-sp1}} = 1) = 0.23$, one-sample t-test; $p(\frac{\text{min}\Delta\text{gt-2-sp1+gt-4}}{\text{minWT-sp1}} > \frac{\text{min}\Delta\text{gt-2-sp1}}{\text{minWT-sp1}}) = 0.17$, one-sided, two-sample t-test with unequal variances).

Methods for details). The expression levels of *eve* stripe 2 in embryos with $\Delta\text{gt-2}$ *eve* locus are not significantly different from those in embryos with WT *eve* locus (p -value = 0.1007, Mann-Whitney *U*-test with Bonferroni correction; Figure 4C). The *eve* stripe 2 patterns driven by the WT *eve* locus and the $\Delta\text{gt-2}$ *eve* locus are also not significantly different (Figure 4B). This suggests that the *gt-2* deletion in the endogenous *eve* stripe 2 enhancer is buffered: expression levels and boundary position in the $\Delta\text{gt-2}$ *eve* locus embryos are not significantly different from the WT *eve* locus embryos, in agreement with the observations made in the extended enhancer. Interestingly, we observed differences between $\Delta\text{gt-2}$ *eve* locus and WT *eve* locus on other stripes of the *eve* pattern (Figure S5). There are differences in the expression levels of *eve* stripes 5 and 6, and in the patterns of *eve* stripe 4 (Figure S5). We speculate that the differences might be due to the effects of the genetic backgrounds of $\Delta\text{gt-2}$ *eve* and WT *eve* locus embryos (see Methods), which is consistent with previous findings of background effects (Lott *et al.* 2007; Kalay *et al.* 2020). All together, these results suggest that the effect of a specific mutation in the *eve*

stripe 2 minimal reporter construct is not recapitulated when tested in the endogenous enhancer context.

DISCUSSION

The desire to define discrete minimal sequences that are sufficient to drive gene expression patterns emerged from a combination of the technical limitations imposed upon early studies and the resulting “founder fallacy” (Halfon 2019), cementing the first discovered examples of enhancers into generalizations. Understanding and acknowledging the ways in which the activity of minimal enhancers in reporter constructs differs from the activity of the same sequences within the endogenous locus will help us understand gene regulatory logic at a genome scale, as well as regulatory variation and evolution. Simultaneously, it also reaffirms the important contributions that reporter constructs can still make to deciphering the mechanisms of transcription (Catarino and Stark 2018).

Using one of the textbook examples of an enhancer, *eve* stripe 2, we have shown that deletion of a key TF binding site for Gt has

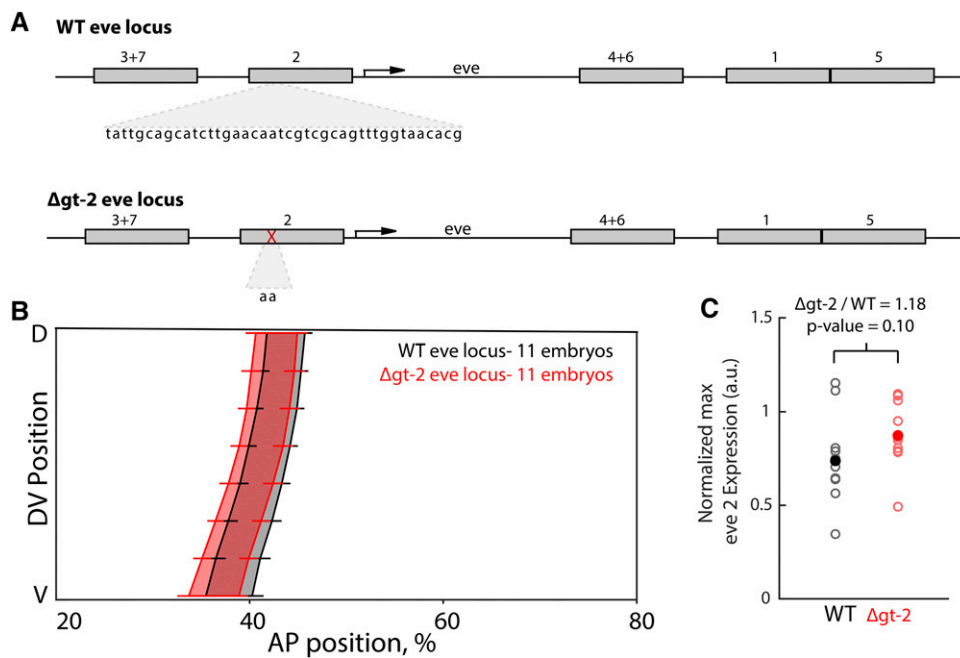


Figure 4 CRISPR deletion of the *gt-2* binding site in endogenous *eve* locus does not change stripe 2 expression. (A) Using a scarless-CRISPR method, we removed the *gt-2* binding site endogenously. (B) The boundaries of *eve* stripe 2 are not significantly different between the Δ gt-2 *eve* locus embryos and the WT locus embryos (Mann-Whitney *U*-test). Error bars show standard error of the mean boundary positions of the expression pattern. This indicates that the boundary of *eve* stripe 2 in the endogenous context is buffered against the removal of *gt-2*. (C) Normalized peak expression levels of *eve* stripe 2 did not change significantly in the Δ gt-2 *eve* locus vs. control ($P = 0.10$, Mann-Whitney *U*-test with Bonferroni adjustment, 8). The ratio of Δ gt-2 *eve* locus to WT *eve* locus equals 1.18. Filled circles represent mean expression level and open circles are *eve* peak expression for each individual embryo analyzed (Δ gt-2 *eve* locus: $n = 11$, WT *eve* locus: $n = 11$).

significant effects on the expression driven by the minimal enhancer sequence, but not when this minimal enhancer is modestly extended, nor when the same binding site is removed from the endogenous locus. Furthermore, we identified an additional Gt binding site found outside the minimal enhancer that contributes to buffering the effect of this mutation.

Given that there were no characterized Gt binding sites in the region flanking the minimal enhancer, it was somewhat unexpected that the effect of the *gt-2* deletion would be buffered in the extended enhancer (Ludwig *et al.* 2011). However, finding all transcription factor binding sites remains a challenge (Keilwagen *et al.* 2019) and may explain why we cannot fully account for the *gt-2* deletion buffering in the extended enhancer (Keilwagen *et al.* 2019). Gt's binding preference has been measured using several techniques, which all yield different sequence motifs (Noyes *et al.* 2008; Li *et al.* 2011; Schroeder *et al.* 2011). We searched for Gt binding sites with three different sequence motifs, and we found and mutated a single high-affinity binding site predicted by all three motifs, *gt-4* (Figure S1). The *gt-4* site is conserved across multiple *Drosophila* species (Figure S7). There are additional predicted Gt binding sites and other conserved regions within these extended sequences that may be contributing to the buffering and to enhancer function.

We do not understand why the minimal spacer constructs that include the *gt-2* deletion show a large anterior shift of the posterior boundary of the expression pattern. The shift is not observed in the wild-type minimal spacer constructs or in the *min* Δ gt-2 or *ext* Δ gt-2 constructs, so it is not due to the spacer sequence or to the *gt-2* deletion individually. We hypothesize there is a specific promoter-enhancer interaction that occurs when both the spacer and the *gt-2* deletion are present, but we cannot speculate on the precise underlying cause of this interaction.

This simple case study illustrates clearly that the effects of mutations, as measured in minimal enhancer sequences, cannot be simply extrapolated to larger enhancer regions or to the enhancer in

its endogenous context in the genome. These results provide additional evidence challenging the idea that enhancers are strictly modular and that they have defined boundaries (Evans *et al.* 2012; Halfon 2019; Sabarís *et al.* 2019). Experiments using minimal enhancer reporter constructs have been extremely valuable for identifying genetic interactions and mechanisms of transcriptional control, *e.g.*, activator/repressor balance and short- and long-range repression (Arnosti *et al.* 1996; Kulkarni and Arnosti 2005; Vincent *et al.* 2018). However, as more high throughput methods are developed to test the effect of mutations in small to medium-size enhancer fragments, we need to be cautious in interpreting these results (Inoue and Ahituv 2015). A mutation that may have dramatic effects on expression when made in a minimal enhancer may have no effect when made in the genome of an organism, which has implications for how we interpret naturally occurring sequence variation in the context of human disease and evolution.

To test the mutation effects definitively, reporter construct experiments need to be complemented with manipulations of the endogenous enhancer sequences. Due to the CRISPR revolution, these types of experiments are becoming increasingly feasible (Zhou *et al.* 2014; Kvon *et al.* 2016; Rogers *et al.* 2017), and methods are being developed to use high-throughput CRISPR experiments to identify and perturb enhancers, as reviewed in (Lopes *et al.* 2016; Catarino and Stark 2018). These experiments will provide the data to attack the challenge of modeling the function of increasingly large pieces of the genome simultaneously, which is ultimately required to predict how variation in enhancer sequences affects gene expression.

ACKNOWLEDGMENTS

We thank all the members of the DePace lab for helpful discussions and suggestions on the manuscript. The research reported in this publication was funded by the Harvard GSAS Research Scholar Initiative (to F.L.R.), NIH grants K99/R00 HD073191 and R01 HD095246 (to Z.W.), the NSF Graduate Research Fellowship

DGE1745303 (to O.K.F.R.), the Giovanni Armenise-Harvard Foundation's HMS Junior Faculty Grants Program, the McKenzie Family Charitable Trust Systems Biology Fellowship Fund, the William F. Milton Fund, the Harriet Sugar Toibin Charitable Gift Annuity – Gene Intervention Research, NSF grants 1715184 and IOS-1452557, NIH grants R21 HD072481, R01 GM122928 and U01 GM103804 (to A.H.D.), and the Novartis fellowship (to J.E.). We thank Jeehae Park for her contribution of the fixed y[1] w[67c23]; attP2{hbp2-LacZ} embryos used in our analyses.

LITERATURE CITED

- Arnold, C. D., D. Gerlach, C. Stelzer, Ł. M. Boryń, M. Rath *et al.*, 2013 Genome-wide quantitative enhancer activity maps identified by STARR-seq. *Science* 339: 1074–1077. <https://doi.org/10.1126/science.1232542>
- Arnosti, D. N., S. Barolo, M. Levine, and S. Small, 1996 The eve stripe 2 enhancer employs multiple modes of transcriptional synergy. *Development* 122: 205–214.
- Barolo, S., 2012 Shadow enhancers: frequently asked questions about distributed cis-regulatory information and enhancer redundancy. *BioEssays* 34: 135–141. <https://doi.org/10.1002/bies.201100121>
- Catarino, R. R., and A. Stark, 2018 Assessing sufficiency and necessity of enhancer activities for gene expression and the mechanisms of transcription activation. *Genes Dev.* 32: 202–223. <https://doi.org/10.1101/gad.310367.117>
- Crocker, J., and D. L. Stern, 2017 Functional regulatory evolution outside of the minimal even-skipped stripe 2 enhancer. *Development* 144: 3095–3101. <https://doi.org/10.1242/dev.149427>
- Diao, Y., R. Fang, B. Li, Z. Meng, J. Yu *et al.*, 2017 A tiling-deletion-based genetic screen for cis-regulatory element identification in mammalian cells. *Nat. Methods* 14: 629–635. <https://doi.org/10.1038/nmeth.4264>
- Evans, N. C., C. I. Swanson, and S. Barolo, 2012 Chapter four - Sparkling Insights into Enhancer Structure, Function, and Evolution, pp. 97–120 in *Current Topics in Developmental Biology*, edited by Plaza, S., and F. Payre. Academic Press, Cambridge, MA.
- Fowlkes, C. C., C. L. L. Hendriks, S. V. E. Keränen, G. H. Weber, O. Rübél *et al.*, 2008 A quantitative spatiotemporal atlas of gene expression in the *Drosophila* blastoderm. *Cell* 133: 364–374. <https://doi.org/10.1016/j.cell.2008.01.053>
- Goto, T., P. Macdonald, and T. Maniatis, 1989 Early and late periodic patterns of even skipped expression are controlled by distinct regulatory elements that respond to different spatial cues. *Cell* 57: 413–422. [https://doi.org/10.1016/0092-8674\(89\)90916-1](https://doi.org/10.1016/0092-8674(89)90916-1)
- Halfon, M. S., 2019 Studying Transcriptional Enhancers: The Founder Fallacy, Validation Creep, and Other Biases. *Trends Genet.* 35: 93–103. <https://doi.org/10.1016/j.tig.2018.11.004>
- Henriques, T., B. S. Scruggs, M. O. Inouye, G. W. Muse, L. H. Williams *et al.*, 2018 Widespread transcriptional pausing and elongation control at enhancers. *Genes Dev.* 32: 26–41. <https://doi.org/10.1101/gad.309351.117>
- Hertz, G. Z., and G. D. Stormo, 1999 Identifying DNA and protein patterns with statistically significant alignments of multiple sequences. *Bioinformatics* 15: 563–577. <https://doi.org/10.1093/bioinformatics/15.7.563>
- Inoue, F., and N. Ahituv, 2015 Decoding enhancers using massively parallel reporter assays. *Genomics* 106: 159–164. <https://doi.org/10.1016/j.ygeno.2015.06.005>
- Kalay, G., J. Atallah, N. C. Sierra, A. M. Tang, A. E. Crofton *et al.*, 2020 Evolution of larval segment position across 12 *Drosophila* species. *Evolution* 74: 1409–1422. <https://doi.org/10.1111/evo.13911>
- Keilwagen, J., S. Posch, and J. Grau, 2019 Accurate prediction of cell type-specific transcription factor binding. *Genome Biol.* 20: 9. <https://doi.org/10.1186/s13059-018-1614-y>
- Koenecke, N., J. Johnston, B. Gaertner, M. Natarajan, and J. Zeitlinger, 2016 Genome-wide identification of *Drosophila* dorso-ventral enhancers by differential histone acetylation analysis. *Genome Biol.* 17: 196. <https://doi.org/10.1186/s13059-016-1057-2>
- Kulkarni, M. M., and D. N. Arnosti, 2005 cis-regulatory logic of short-range transcriptional repression in *Drosophila melanogaster*. *Mol. Cell. Biol.* 25: 3411–3420. <https://doi.org/10.1128/MCB.25.9.3411-3420.2005>
- Kvon, E. Z., O. K. Kamneva, U. S. Melo, I. Barozzi, M. Osterwalder *et al.*, 2016 Progressive Loss of Function in a Limb Enhancer during Snake Evolution. *Cell* 167: 633–642.e11. <https://doi.org/10.1016/j.cell.2016.09.028>
- Kwasnieski, J. C., C. Fiore, H. G. Chaudhari, and B. A. Cohen, 2014 High-throughput functional testing of ENCODE segmentation predictions. *Genome Res.* 24: 1595–1602. <https://doi.org/10.1101/gr.173518.114>
- Li, X.-Y., S. Thomas, P. J. Sabo, M. B. Eisen, J. A. Stamatoyannopoulos *et al.*, 2011 The role of chromatin accessibility in directing the widespread, overlapping patterns of *Drosophila* transcription factor binding. *Genome Biol.* 12: R34. <https://doi.org/10.1186/gb-2011-12-4-r34>
- Li, X.-Y., and M. B. Eisen, 2018 Mutation of sequences flanking and separating transcription factor binding sites in a *Drosophila* enhancer significantly alter its output. *bioRxiv Preprint* posted July 30, 2018.
- Lim, B., T. Fukaya, T. Heist, and M. Levine, 2018 Temporal dynamics of pair-rule stripes in living *Drosophila* embryos. *Proc. Natl. Acad. Sci. USA* 115: 8376–8381. <https://doi.org/10.1073/pnas.1810430115>
- Lopes, R., G. Korkmaz, and R. Agami, 2016 Applying CRISPR-Cas9 tools to identify and characterize transcriptional enhancers. *Nat. Rev. Mol. Cell Biol.* 17: 597–604. <https://doi.org/10.1038/nrm.2016.79>
- Lott, S. E., M. Kreitman, A. Palsson, E. Alekseeva, and M. Z. Ludwig, 2007 Canalization of segmentation and its evolution in *Drosophila*. *Proc. Natl. Acad. Sci. USA* 104: 10926–10931. <https://doi.org/10.1073/pnas.0701359104>
- Ludwig, M. Z., R. Manu, K. P. White and M. Kreitman, 2011 Consequences of eukaryotic enhancer architecture for gene expression dynamics, development, and fitness. *PLoS Genet.* 7: e1002364. <https://doi.org/10.1371/journal.pgen.1002364>
- Ludwig, M. Z., N. H. Patel, and M. Kreitman, 1998 Functional analysis of eve stripe 2 enhancer evolution in *Drosophila*: rules governing conservation and change. *Development* 125: 949–958.
- Luengo Hendriks, C. L., S. V. E. Keränen, C. C. Fowlkes, L. Simirenko, G. H. Weber *et al.*, 2006 Three-dimensional morphology and gene expression in the *Drosophila* blastoderm at cellular resolution I: data acquisition pipeline. *Genome Biol.* 7: R123. <https://doi.org/10.1186/gb-2006-7-12-r123>
- Ma, L., J. Merenmies, and L. F. Parada, 2000 Molecular characterization of the TrkA/NGF receptor minimal enhancer reveals regulation by multiple cis elements to drive embryonic neuron expression. *Development* 127: 3777–3788.
- Melnikov, A., A. Murugan, X. Zhang, T. Tesileanu, L. Wang *et al.*, 2012 Systematic dissection and optimization of inducible enhancers in human cells using a massively parallel reporter assay. *Nat. Biotechnol.* 30: 271–277. <https://doi.org/10.1038/nbt.2137>
- Milewski, R. C., N. C. Chi, J. Li, C. Brown, M. M. Lu *et al.*, 2004 Identification of minimal enhancer elements sufficient for Pax3 expression in neural crest and implication of Tead2 as a regulator of Pax3. *Development* 131: 829–837. <https://doi.org/10.1242/dev.00975>
- Monti, R., I. Barozzi, M. Osterwalder, E. Lee, M. Kato *et al.*, 2017 Limb-Enhancer Genie: An accessible resource of accurate enhancer predictions in the developing limb. *PLOS Comput. Biol.* 13: e1005720. <https://doi.org/10.1371/journal.pcbi.1005720>
- Ney, P. A., B. P. Sorrentino, K. T. McDonagh, and A. W. Nienhuis, 1990 Tandem AP-1-binding sites within the human beta-globin dominant control region function as an inducible enhancer in erythroid cells. *Genes Dev.* 4: 993–1006. <https://doi.org/10.1101/gad.4.6.993>
- Noyes, M. B., X. Meng, A. Wakabayashi, S. Sinha, M. H. Brodsky *et al.*, 2008 A systematic characterization of factors that regulate *Drosophila* segmentation via a bacterial one-hybrid system. *Nucleic Acids Res.* 36: 2547–2560. <https://doi.org/10.1093/nar/gkn048>
- Patwardhan, R. P., C. Lee, O. Litvin, D. L. Young, D. Pe'er *et al.*, 2009 High-resolution analysis of DNA regulatory elements by synthetic saturation mutagenesis. *Nat. Biotechnol.* 27: 1173–1175. <https://doi.org/10.1038/nbt.1589>

- Petkova, M. D., G. Tkačik, W. Bialek, E. F. Wieschaus, and T. Gregor, 2019 Optimal Decoding of Cellular Identities in a Genetic Network. *Cell* 176: 844–855.e15. <https://doi.org/10.1016/j.cell.2019.01.007>
- Rogers, W. A., Y. Goyal, K. Yamaya, S. Y. Shvartsman, and M. S. Levine, 2017 Uncoupling neurogenic gene networks in the *Drosophila* embryo. *Genes Dev.* 31: 634–638. <https://doi.org/10.1101/gad.297150.117>
- Rohs, R., X. Jin, S. M. West, R. Joshi, B. Honig *et al.*, 2010 Origins of specificity in protein-DNA recognition. *Annu. Rev. Biochem.* 79: 233–269. <https://doi.org/10.1146/annurev-biochem-060408-091030>
- Sabaris, G., I. Laiker, E. Preger-Ben Noon, and N. Frankel, 2019 Actors with Multiple Roles: Pleiotropic Enhancers and the Paradigm of Enhancer Modularity. *Trends Genet.* 35: 423–433. <https://doi.org/10.1016/j.tig.2019.03.006>
- Schroeder, M. D., C. Greer, and U. Gaul, 2011 How to make stripes: deciphering the transition from non-periodic to periodic patterns in *Drosophila* segmentation. *Development* 138: 3067–3078. <https://doi.org/10.1242/dev.062141>
- Shlyueva, D., G. Stampfel, and A. Stark, 2014 Transcriptional enhancers: from properties to genome-wide predictions. *Nat. Rev. Genet.* 15: 272–286. <https://doi.org/10.1038/nrg3682>
- Small, S., A. Blair, and M. Levine, 1992 Regulation of even-skipped stripe 2 in the *Drosophila* embryo. *EMBO J.* 11: 4047–4057. <https://doi.org/10.1002/j.1460-2075.1992.tb05498.x>
- Spitz, F., and E. E. M. Furlong, 2012 Transcription factors: from enhancer binding to developmental control. *Nat. Rev. Genet.* 13: 613–626. <https://doi.org/10.1038/nrg3207>
- Staller, M. V., C. C. Fowlkes, M. D. J. Bragdon, Z. Wunderlich, J. Estrada *et al.*, 2015 A gene expression atlas of a bicoid-depleted *Drosophila* embryo reveals early canalization of cell fate. *Development* 142: 587–596. <https://doi.org/10.1242/dev.117796>
- Vincent, B. J., M. V. Staller, F. Lopez-Rivera, M. D. J. Bragdon, E. C. G. Pym *et al.*, 2018 Hunchback is counter-repressed to regulate even-skipped stripe 2 expression in *Drosophila* embryos. *PLoS Genet.* 14: e1007644. <https://doi.org/10.1371/journal.pgen.1007644>
- White, M. A., 2015 Understanding how cis-regulatory function is encoded in DNA sequence using massively parallel reporter assays and designed sequences. *Genomics* 106: 165–170. <https://doi.org/10.1016/j.ygeno.2015.06.003>
- Wunderlich, Z., M. D. Bragdon, and A. H. DePace, 2014 Comparing mRNA levels using in situ hybridization of a target gene and co-stain. *Methods* 68: 233–241. <https://doi.org/10.1016/j.ymeth.2014.01.003>
- Zhou, H. Y., Y. Katsman, N. K. Dhaliwal, S. Davidson, N. N. Macpherson *et al.*, 2014 A Sox2 distal enhancer cluster regulates embryonic stem cell differentiation potential. *Genes Dev.* 28: 2699–2711. <https://doi.org/10.1101/gad.248526.114>

Communicating editor: S. Lott